

## COUPLED NASTRAN/BOUNDARY ELEMENT FORMULATION FOR ACOUSTIC SCATTERING

by

Gordon C. Everstine and Francis M. Henderson  
Numerical Mechanics Division (184)  
David Taylor Naval Ship R&D Center  
Bethesda, Maryland 20084

and

Luise S. Schuetz  
Physical Acoustics Branch (5130)  
Naval Research Laboratory  
Washington, DC 20375

## ABSTRACT

A coupled finite element/boundary element capability is described for calculating the sound pressure field scattered by an arbitrary submerged 3-D elastic structure. Structural and fluid impedances are calculated with no approximation other than discretization. The surface fluid pressures and normal velocities are first calculated by coupling a NASTRAN finite element model of the structure with a discretized form of the Helmholtz surface integral equation for the exterior fluid. Far-field pressures are then evaluated from the surface solution using the Helmholtz exterior integral equation. The overall approach is illustrated and validated using a known analytic solution for scattering from submerged spherical shells.

## INTRODUCTION

Two fundamental problems of interest in structural acoustics are the calculation of the far-field acoustic pressure field radiated by a general submerged three-dimensional elastic structure subjected to internal time-harmonic loads and the calculation of the far-field acoustic pressure scattered by an elastic structure subjected to an incident time-harmonic wave train. These problems are usually solved by combining a finite element model of the structure with a fluid loading computed using either finite element [1-3] or boundary integral equation [4-11] techniques.

Although both approaches are computationally expensive for large structural models, the fluid finite element approach is burdened with the additional complications caused by the approximate radiation boundary condition at the outer fluid boundary, the requirements on mesh size and extent, and the difficulty of generating the fluid mesh [1,3].

In contrast, the boundary integral equation (BIE) approach for generating the fluid loading is mathematically exact (except for surface discretization error) and requires little or no additional modeling effort to convert an existing model of a dry structure for use in submerged analyses. The saving in engineering time, however, is partially offset by the somewhat greater computing costs associated with the BIE approach.

Several general BIE acoustic radiation capabilities have been developed previously [4, 7, 11]. One, called NASHUA [11], couples a NASTRAN finite element model of a dry structure with a fluid loading calculated by a discretized form of the Helmholtz surface integral equation. NASHUA is the only capability developed for a widely-used, public domain, general purpose structural analysis code. Here we present an extension to NASHUA to handle also the problem of acoustic scattering from general three-dimensional elastic structures.

The primary purposes of this paper are to summarize the theoretical basis for NASHUA and to demonstrate its validity for scattering by showing results of calculations for the elementary problem of plane-wave scattering from a thin spherical shell.

#### THEORETICAL APPROACH

Consider an arbitrary submerged 3-D elastic structure subjected to either internal time-harmonic loads or an external time-harmonic incident pressure wave train. The matrix equation of motion for the structural degrees of freedom (DOF) can be written as

$$Zv = F - GA p \quad (1)$$

where  $Z$  = structural impedance matrix (dimension  $s \times s$ ),  
 $v$  = complex amplitude of the velocity vector for all structural DOF (wet or dry) in terms of the coordinate systems selected by the user ( $s \times r$ ),  
 $F$  = complex amplitude of the vector of mechanical forces applied to the structure ( $s \times r$ ),  
 $G$  = rectangular transformation matrix of direction cosines to transform a vector of outward normal forces at the wet points to a vector of forces at all points in the coordinate systems selected by the user ( $s \times f$ ),  
 $A$  = diagonal area matrix for the wet surface ( $f \times f$ ), and  
 $p$  = complex amplitude of total pressures (incident + scattered) applied at the wet grid points ( $f \times r$ ).

In this equation, the time dependence  $\exp(i\omega t)$  has been suppressed. In the above dimensions,  $s$  denotes the total number of structural DOF (wet or dry),  $f$  denotes the number of fluid DOF (the number of wet points), and  $r$  denotes the number of load cases. In general, surface areas in NASHUA are obtained

from the NASTRAN calculation of the load vector resulting from an outwardly directed static unit pressure load on the structure's wet surface.

In Equation (1), the structural impedance matrix  $Z$  (the ratio of force to velocity) is given by

$$Z = (-\omega^2 M + i\omega B + K)/i\omega \quad (2)$$

where  $M$ ,  $B$ , and  $K$  are the structural mass, viscous damping, and stiffness matrices, respectively, and  $\omega$  is the circular frequency of excitation. For structures with material damping or a nonzero loss factor,  $K$  is complex.

The total fluid pressure  $p$  satisfies the reduced wave equation

$$\nabla^2 p + k^2 p = 0 \quad (3)$$

where  $k = \omega/c$  is the acoustic wave number, and  $c$  is the speed of sound in the fluid. Equivalently,  $p$  is the solution of the Helmholtz integral equation [7,12]

$$\int_S p(\underline{x})(\partial D(r)/\partial n) dS - \int_S q(\underline{x}) D(r) dS = \begin{cases} p(\underline{x}')/2 - p_I, & \underline{x}' \text{ on } S \\ p(\underline{x}') - p_I, & \underline{x}' \text{ in } E \end{cases} \quad (4)$$

where  $S$  and  $E$  denote surface and exterior fluid points, respectively,  $p_I$  is the incident free-field pressure,  $r$  is the distance from  $\underline{x}$  to  $\underline{x}'$  (Figure 1),

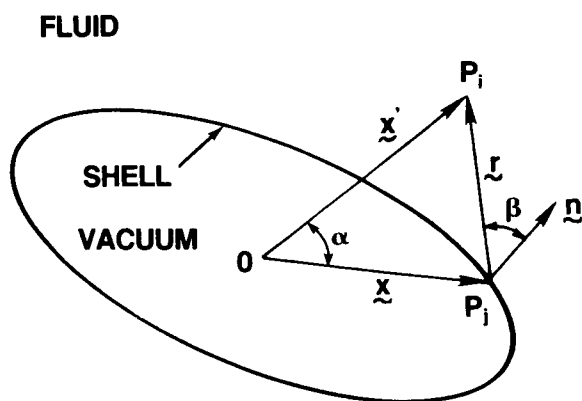


Figure 1 - Notation for Helmholtz Integral Equations

D is the Green's function

$$D(\underline{r}) = e^{-ikr}/4\pi r \quad (5)$$

and

$$q = \partial p / \partial n = -i\omega\rho v_n \quad (6)$$

where  $\rho$  is the density of the fluid, and  $v_n$  is the outward normal component of velocity on S. As shown in Figure 1,  $\underline{x}$  in Equation (4) is the position vector for a typical point  $P_j$  on the surface S,  $\underline{x}'$  is the position vector for the point  $P_i$  which may be either on the surface or in the exterior field E, the vector  $\underline{r} = \underline{x}' - \underline{x}$ , and  $\underline{n}$  is the unit outward normal at  $P_j$ . We denote the lengths of the vectors  $\underline{x}$ ,  $\underline{x}'$ , and  $\underline{r}$  by  $x$ ,  $x'$ , and  $r$ , respectively. The normal derivative of the Green's function D appearing in Equation (4) can be evaluated as

$$\partial D(\underline{r}) / \partial n = (e^{-ikr}/4\pi r) (ik + 1/r) \cos \beta \quad (7)$$

where  $\beta$  is defined as the angle between the normal  $\underline{n}$  and the vector  $\underline{r}$ , as shown in Figure 1.

The substitution of Equations (6) and (7) into the surface equation (4) yields

$$\begin{aligned} p(\underline{x}')/2 - \int_S p(\underline{x}) (e^{-ikr}/4\pi r) (ik + 1/r) \cos \beta \, dS \\ = i\omega\rho \int_S v_n(\underline{x}) (e^{-ikr}/4\pi r) dS + p_I \end{aligned} \quad (8)$$

where  $\underline{x}'$  is on S. This equation is an integral equation relating the total pressure  $p$  and normal velocity  $v_n$  on S. If the integrals in Equation (8) are discretized for numerical computation (the details of which were presented previously [11]), we obtain the matrix equation

$$Ep = Cv_n + p_I \quad (9)$$

on S, where  $p$  is the vector of complex amplitudes of the total pressure on the structure's surface,  $E$  and  $C$  are fully-populated, complex, non-symmetric, frequency-dependent matrices, and  $p_I$  is the complex amplitude of the incident pressure vector (if any). The number of unknowns in this system is  $f$ , the number of wet points on the fluid-structure interface.

The normal velocities  $v_n$  in Equation (9) are related to the total velocities  $v$  by the same transformation matrix  $G$ :

$$v_n = G^T v \quad (10)$$

where  $T$  denotes the matrix transpose. If velocities  $v$  and  $v_n$  are eliminated from Equations (1), (9), and (10), the resulting equation for the coupled fluid-structure system is

$$H p = Q + p_I \quad (11)$$

where

$$H = E + C G^T Z^{-1} G A \quad (12)$$

and

$$Q = C G^T Z^{-1} F \quad (13)$$

Since  $H$  and  $Q$  depend on geometry, material properties, and frequency, Equation (11) may be solved to yield the total surface pressures  $p$ . The vector  $v$  of velocities at all structural DOF may be recovered by solving Equation (1) for  $v$ :

$$v = Z^{-1} F - Z^{-1} G A p \quad (14)$$

Surface normal velocities  $v_n$  may then be recovered by substituting this solution for  $v$  into Equation (10). The triangular factors of  $Z$  are saved when first generated in Equation (12) and reused in Equations (13) and (14).

The free-field incident pressure for planar or spherical waves is calculated in the following way. Consider an arbitrary surface  $S$  subjected to a time-harmonic incident wave train of speed  $c$  and circular frequency  $\omega$  as shown in Figure 2. The complex amplitude  $p_I$  of the incident pressure at a typical point  $i$  is given by

$$p_I = \begin{cases} p_0 \exp(i\theta_i), & \text{plane wave} \\ p_0 \exp(i\theta_i) s / (s - \delta_i), & \text{spherical wave} \end{cases} \quad (15)$$

where  $p_0$  is the pressure amplitude at the coordinate origin (where the phase angle is arbitrarily set to zero),  $s$  is the length of the vector  $\underline{s}$  (the vector from the origin to the source),  $\delta_i$  is the distance (positive or negative)

from the origin to the wavefront through point  $i$ , and  $\theta_i$  is the phase angle for point  $i$ . These last two quantities can be computed using

$$\theta_i = k \delta_i \quad (16)$$

and

$$\delta_i = \begin{cases} \underline{x}_i \cdot \underline{s}/s, & \text{plane wave} \\ s - |\underline{x}_i - \underline{s}|, & \text{spherical wave} \end{cases} \quad (17)$$

where  $\underline{x}_i$  is the position vector for point  $i$ . For plane waves, only the direction cosines of  $\underline{s}$  are used. Positive values of  $\theta_i$  and  $\delta_i$  for a point  $i$  correspond to that point's being closer to the source than the origin is.

To summarize, the NASHUA solution procedure uses NASTRAN to generate  $K$ ,  $M$ ,  $B$ , and  $F$  and to generate sufficient geometry information so that  $E$ ,  $C$ ,  $G$ ,  $A$ , and  $p_i$  can be computed by a separate program (SURF). Then, given all matrices on the right-hand sides of Equations (12) and (13), NASTRAN DMAP is used to compute  $H$  and  $Q$ . Equation (11) is then solved for the surface pressures  $p$  using a new block solver (OCSOLVE) written especially for this problem by E.A. Schroeder of the David Taylor Naval Ship R&D Center. Next, NASTRAN DMAP is used to recover the surface normal velocities  $v_n$  and the vector  $v$  of velocities at all structural DOF. This completes the surface solution. In general, this approach combines in a highly automated fashion a finite element model of the structure with a Helmholtz boundary integral equation model of the fluid.

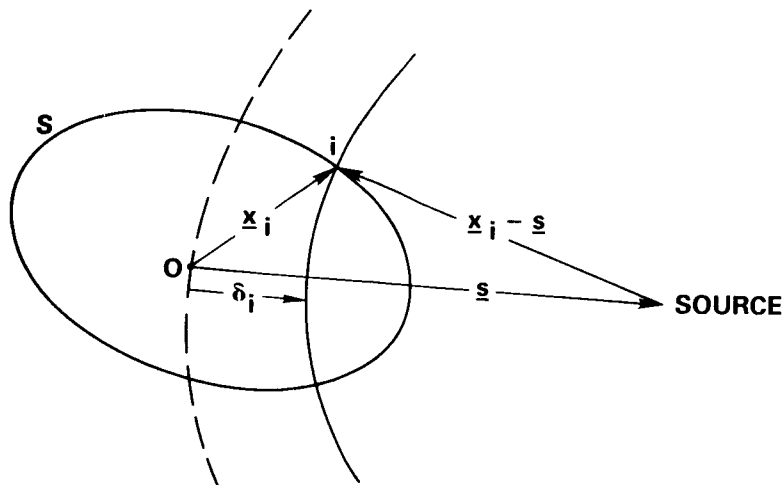


Figure 2 - Geometry for Calculating Incident Pressure

### The Far-Field Solution

Given the solution for the total pressures and velocities on the surface, the exterior Helmholtz integral equation, Equation (4), can be integrated to obtain the radiated (or scattered) pressure at any desired location  $\underline{x}'$  in the field. We first substitute Equations (6) and (7) into Equation (4) to obtain a form suitable for numerical integration:

$$p(\underline{x}') = \int_S [i\omega\rho v_n(\underline{x}) + (ik + 1/r)p(\underline{x}) \cos \beta] (e^{-ikr}/4\pi r) dS \quad (18)$$

where all symbols have the same definitions as were used previously, and  $\underline{x}'$  is in the exterior field. Thus, given the total pressure  $p$  and normal velocity  $v_n$  on the surface  $S$ , the radiated or scattered pressure at  $\underline{x}'$  can be determined by numerical quadrature using Equation (18).

In applications, however, the field pressures generally of interest are in the far-field, so we use instead an asymptotic (far-field) form [11] of Equation (18):

$$p(\underline{x}') = (ike^{-ikx'}/4\pi x') \int_S [\rho c v_n(\underline{x}) + p(\underline{x}) \cos \beta] e^{ikx \cos \alpha} dS \quad (19)$$

where  $\alpha$  is the angle between the vectors  $\underline{x}$  and  $\underline{x}'$  (Figure 1), and, for far-field points,  $\cos \beta$  is computed using

$$\cos \beta = \underline{n} \cdot \underline{x}'/x' \quad (20)$$

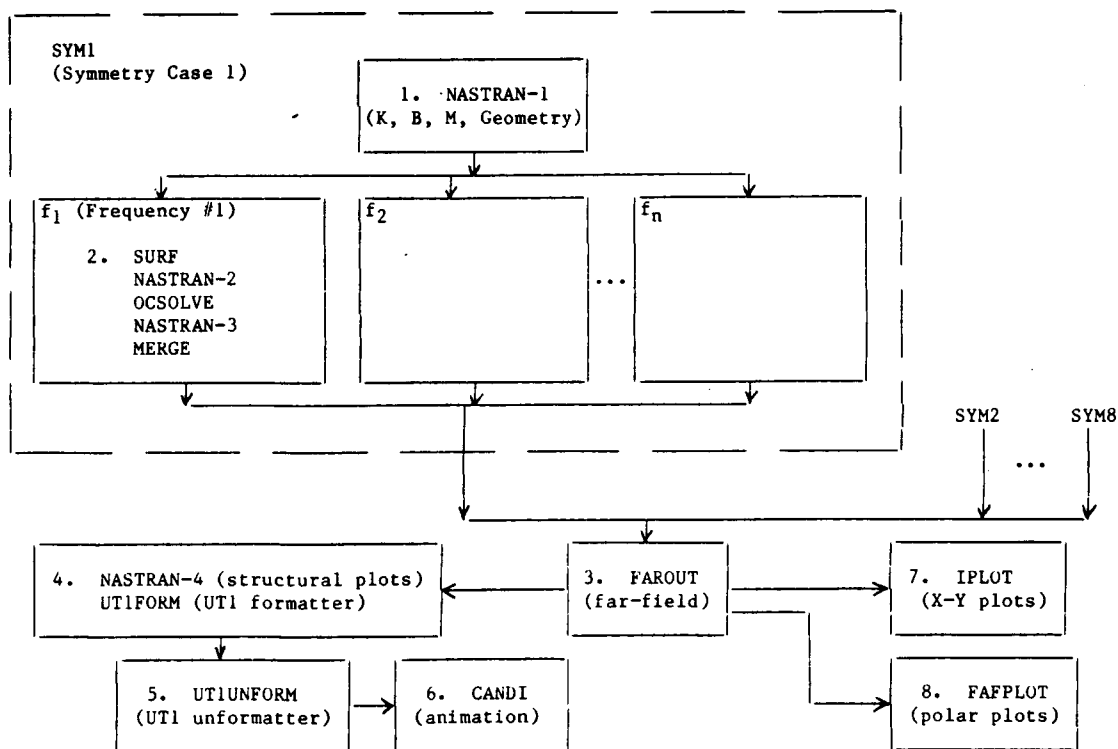
We note that, since Equation (19) is a far-field formula, the pressure varies inversely with distance  $x'$  everywhere so that any range  $x'$  may be used in its evaluation (e.g., 36 inches).

### OVERVIEW OF NASHUA SOLUTION PROCEDURE

The overall organization and setup of the solution procedure is summarized in Figure 3. NASTRAN appears four times in the procedure; to distinguish one NASTRAN execution from another, the integers 1-4 are appended to "NASTRAN" in the figure.

A separate NASTRAN model is prepared and run (Step 1 in Figure 3) for each unique set of symmetry constraints. Since up to three planes of reflective symmetry are allowed, there would be one, two, four, or eight such runs. Step 1 generates files containing geometry information and a checkpoint file for subsequent use in the other steps.

For each symmetry case and drive frequency, the Step 2 sequence is run in a single job. The SURF program reads the geometry file generated by NASTRAN in Step 1 and, using the Helmholtz surface integral equation, generates the fluid matrices E and C for the exterior fluid, the area matrix A, the structure-fluid transformation matrix G, the free-field incident pressure vector  $p_I$ , and a geometry file to be used later by FAROUT (Step 3) for the field calculation. SURF is followed by a NASTRAN job which takes the matrices K, M, B, and F from Step 1 and the matrices E, C, A, and G from SURF and calculates H and Q according to Equations (12) and (13). Equation (11) is then solved for the surface pressure vector p by program OCSOLVE written by E.A. Schroeder of DTNSRDC. OCSOLVE is a general block solver for full, complex, nonsymmetric systems of linear, algebraic equations. The program was designed to be particularly effective on such systems and executes about 20 times faster than NASTRAN's equation solver, which was not designed for efficient solution of such systems of equations. NASTRAN is then re-entered in Step 2 with p so that the velocities  $v$  and  $v_n$  can be recovered using DMAP operations according to Equations (14) and (10), respectively.



NOTE: Each solid block is a separate job submission.

Figure 3 - Summary of NASHUA Solution Procedure



The surface pressures, normal velocities, and full g-set displacements are then reformatted and merged into a single file (for each symmetry case) using program MERGE.

Steps 1 and 2 are repeated for each symmetry case. After all symmetry cases have been completed and merged, program FAROUT (Step 3) is run to combine the symmetry cases and to integrate over the surface. FAROUT uses as input the geometry file generated by SURF (Step 2) and the surface solutions from the one, two, four, or eight symmetry cases generated by MERGE. The far-field pressure solution is obtained by integrating the surface pressures and velocities using the far-field form of the exterior Helmholtz integral equation, Equation (19). Output from FAROUT consists of both tables and files suitable for various types of plotting.

The remaining steps in the NASHUA procedure are for graphical display. Deformed structural plots of the frequency response may be obtained by restarting NASTRAN (Step 4) with the checkpoint file from Step 1 and a results file from FAROUT. In addition, animated plots can be generated on the Evans & Sutherland PS-330 graphics terminal using the CANDI program (Step 6) written for the DEC/VAX computer by R.R. Lipman of DTNSRDC [13]. If the rest of NASHUA is run on a computer other than the VAX, the NASTRAN UT1 file which is passed to CANDI must first be formatted (Step 4) for transfer to the VAX computer and then unformatted (Step 5) for reading by CANDI.

X-Y plots of various quantities (both surface and far-field) versus frequency may be obtained using the general purpose interactive plotting program IPLOT [14] (Step 7). Polar plots of the far-field sound pressure levels in each of the three principal coordinate planes can also be generated using the interactive graphics program FAFLOT [15] (Step 8) written by R.R. Lipman of DTNSRDC.

#### FREQUENCY LIMITATIONS

It is known that the fluid matrices E and C in the surface Helmholtz integral equation formulation are singular at the frequencies of the resonances of the corresponding interior acoustic cavity with Dirichlet (zero pressure) boundary conditions [5]. Although the NASHUA formulation described in the previous section was designed to avoid having to invert either E or C in Equations (12) and (13), the coefficient matrix H is also poorly conditioned at these frequencies (referred to as the "critical" or "forbidden" frequencies of the problem) [11]. Therefore, to be safe, the user should generally avoid excitation frequencies which exceed the lowest critical frequency for the geometry in question.

For spheres, for example, the lowest critical frequency occurs at  $ka = \pi$ , where k is the acoustic wave number, and a is the radius. For long cylinders with flat ends, the lowest critical frequency occurs at  $ka \approx 2.4$ , where a is the radius. For short cylinders with flat ends, the lowest critical frequency is slightly higher than for long cylinders.

## RESTRICTIONS ON MODEL

Although the NASHUA solution procedure was designed to be general enough so that arbitrary three-dimensional structures could be analyzed, a few restrictions remain. In our view, however, none is a burden, since a NASTRAN deck for a dry structure modeled with low-order finite elements can usually be adapted for use with NASHUA in a few hours. The following general restrictions apply:

1. All translational degrees of freedom (DOF) for wet points must be in NASTRAN's "analysis set" (a-set), since all symmetry cases must have the same wet DOF, and the fluid matrices E and C involve all wet points. This restriction also affects constraints. Thus, constraints on translational DOF of wet points may not be imposed with single point constraint (SPC) cards, but must instead be imposed using large springs connected between the DOF to be constrained and ground. Generally, this restriction affects only those DOF which are constrained due to symmetry conditions.
2. The wet face of each finite element in contact with the exterior fluid must be defined by either three or four grid points, since the numerical discretization of the Helmholtz surface integral equation assumes the use of low order elements. In particular, NASTRAN elements with midside nodes (e.g., TRIM6, IS2D8, or IHEX2) may not be in contact with the exterior fluid.
3. Symmetry planes must be coordinate planes of the basic Cartesian coordinate system.
4. No scalar points or extra points are allowed, since program SURF assumes that each point is a grid point.
5. For cylindrical shells, the axis of the cylinder should coincide with one of the three basic Cartesian axes; for spherical shells, the center of the sphere should coincide with the basic origin. These restrictions facilitate the treatment of symmetry planes and the calculation of curvatures in program SURF.
6. At least one degree of freedom in the model should be constrained with an SPC, MPC, or OMIT card so that the NASTRAN data block PL is generated.
7. Thin structures with fluid on both sides should be avoided, since the formulations for the fluid matrices are singular if two wet points are coincident. A precise restriction is not known.

## TIME ESTIMATION

On CDC computers, most of the computer time required to execute the entire NASHUA procedure is associated with the forward/backward solve (FBS) operation in Step 2, Equation (12), in which the matrix  $Z^{-1}GA$  is computed given the triangular factors of Z and the matrix GA. Z is a complex, symmetric, banded matrix of dimension  $s \times s$ , where s is the number of structural DOF in the problem, and GA is a real, sparsely-populated,

rectangular matrix of dimension  $s \times f$ , where  $f$  is the number of fluid DOF (the number of wet points on the surface). This FBS time is proportional to the product of  $s$ ,  $f$ , and  $W_{avg}$  (the average wavefront for the stiffness matrix  $K$ ), and, for large jobs, accounts for a substantial part (perhaps two-thirds) of the total time to make a single pass through the NASHUA Step 2 procedure.

For example, consider a problem with the following characteristics:

$s = 2973$  (number of structural DOF)  
 $f = 496$  (number of fluid DOF)  
 $W_{avg} = 129$  (average wavefront of stiffness matrix)

On the CDC Cyber 176 computer at DTNSRDC, the computer time ("wall-clock" time) required to solve this problem in a dedicated computer environment for a single symmetry case and one drive frequency was about 30 minutes, of which 19 minutes were spent in the FBS operation.

#### PROGRAM VALIDATION

For radiation problems, NASHUA has been validated previously [11] for submerged spherical shells driven internally by both uniform and non-uniform (sector) pressure loads. Here we demonstrate NASHUA's ability to solve scattering problems by solving the problem of the submerged thin spherical shell subjected to an incident time-harmonic planar wave train, as shown in Figure 4. The solution of this problem exhibits rotational symmetry about the spherical axis parallel to the direction of wave propagation. The benchmark solution to which the NASHUA results will be compared is a series solution published in the Junger and Feit book [16].

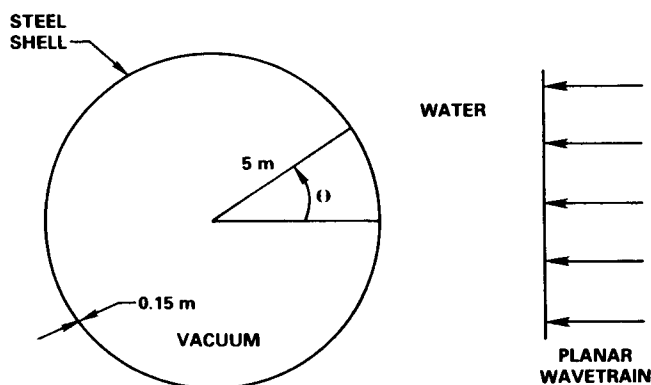


Figure 4 - Plane Wave Scattering from an Elastic Spherical Shell

The problem to be solved has the following characteristics [17]:

$a = 5$ m	(shell radius)
$h = 0.15$ m	(shell thickness)
$E = 2.07 \times 10^{11}$ Pa	(Young's modulus)
$\nu = 0.3$	(Poisson's ratio)
$\rho_s = 7669$ kg/m <sup>3</sup>	(shell density)
$\eta = 0$	(shell loss factor)
$\rho = 1000$ kg/m <sup>3</sup>	(fluid density)
$c = 1524$ m/s	(fluid speed of sound)

One octant of the shell was modeled with NASTRAN's CTRIA2 membrane/bending elements as shown in Figure 5. With 20 elements along each edge of the domain, the model has 231 wet points and 1263 structural DOF. Since the incident loading does not exhibit three planes of symmetry, the NASHUA solution of this problem requires decomposing the solution into both symmetric and antisymmetric parts of the problem, thus providing a good check on NASHUA's ability to combine symmetry cases for scattering problems.

The NASHUA model was run for 15 different drive frequencies in the nondimensional frequency range  $ka = 0.5$  to  $ka = 5.0$ , where  $a$  is the shell radius. Two of the excitation frequencies are near a critical frequency. (The first 13 critical frequencies are located at  $ka = \pi, 4.49, 5.76, 2\pi, 6.99, 7.73, 8.18, 9.10, 9.36, 3\pi, 10.4, 10.5$ , and  $10.9$  [18].) Figure 6 shows a comparison between the NASHUA calculations and the series solution for the far-field scattered pressure in the forward direction ( $\theta = 180$  degrees).

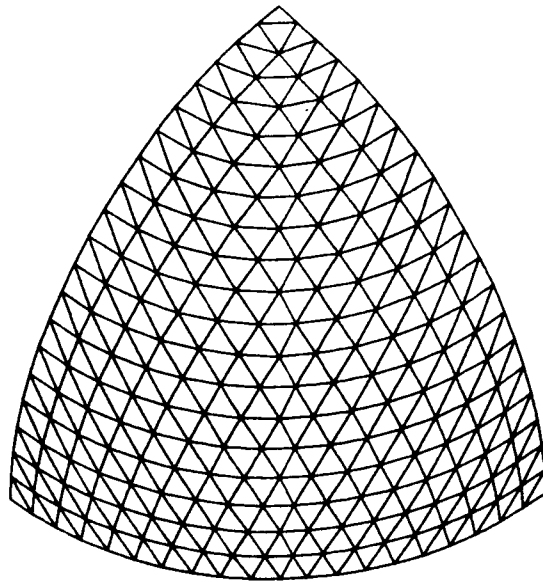


Figure 5 - Finite Element Model of One Octant of Spherical Shell

The ordinate of this figure is the normalized pressure  $|p_r/p_0a|$ , where  $p_r$  is the far-field scattered pressure at distance  $r$  from the origin, and  $p_0$  is the magnitude of the incident pressure. Clearly, the NASHUA solution agrees very well with the exact (i.e., converged series) solution. We note that the NASHUA calculation at  $ka = 4.5$  is adversely affected by the forbidden frequency at  $ka = 4.49$ . (Often, the effect of a forbidden frequency is very severe [11].) For several of the excitation frequencies, we also tabulate on the next page the far-field scattered pressure patterns. Again the agreement between the NASHUA calculations and the series solution is excellent, even at  $ka = 1.6$ , which is near a resonant peak. At the sharper resonant peaks, the results would be much more sensitive to small changes in frequency.

#### DISCUSSION

A very general capability has been described for predicting the acoustic sound pressure field scattered by arbitrary three-dimensional elastic structures subjected to time-harmonic incident loads. Sufficient automation is provided so that, for many structures of practical interest, an existing

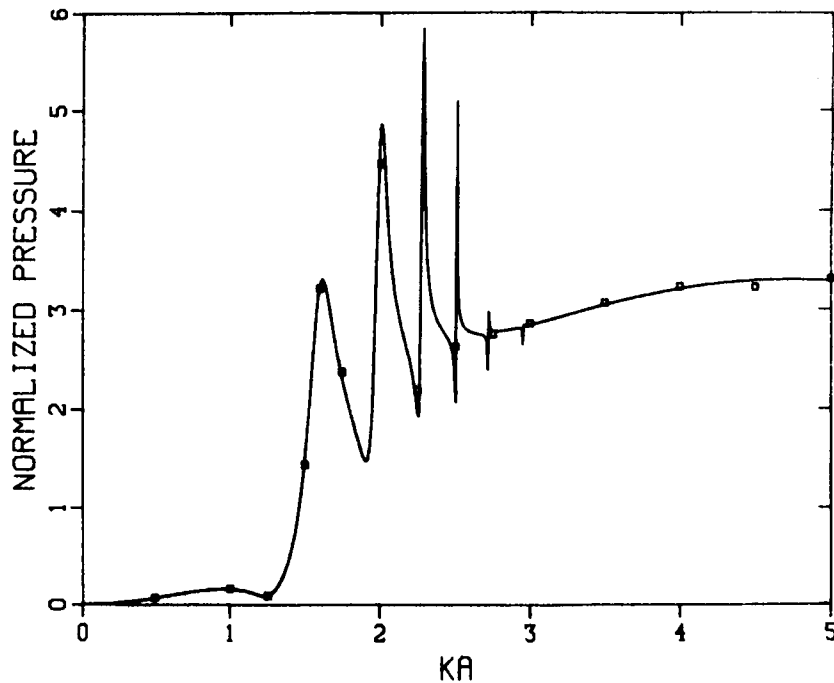


Figure 6 - Normalized Far-Field Pressure  $|p_r/p_0a|$  Scattered in the Forward Direction ( $\theta = 180$  degrees) by a Spherical Shell; Solid Curve is Converged Series Solution [16], and Square Boxes are NASHUA Solution.

Table - Comparison of NASHUA Solution with Converged Series  
Solution for Scattering from Spherical Shell

ka	Angle $\theta$ (degrees)	Normalized Far-Field Pressure, $p_{rr}/p_{0a}$		
		NASHUA	Exact	% Error
0.5	0*	0.0083	0.0081	2.5
	30	0.0144	0.0143	0.7
	60	0.0299	0.0299	0.0
	90	0.0481	0.0481	0.0
	120	0.0626	0.0626	0.0
	150	0.0708	0.0708	0.0
	180	0.0734	0.0733	0.1
1.0	0*	0.0892	0.0903	1.2
	30	0.0382	0.0389	1.8
	60	0.0886	0.0886	0.0
	90	0.1926	0.1930	0.2
	120	0.2208	0.2210	0.1
	150	0.1893	0.1887	0.3
	180	0.1662	0.1652	0.6
1.6	0*	3.146	3.149	0.1
	30	1.993	1.995	0.1
	60	0.325	0.320	1.6
	90	1.515	1.498	1.1
	120	0.561	0.540	3.9
	150	2.058	2.092	1.6
	180	3.213	3.245	1.0
4.0	0*	0.166	0.160	3.8
	30	0.105	0.101	4.0
	60	0.068	0.069	1.4
	90	0.274	0.269	1.9
	120	0.562	0.554	1.4
	150	1.769	1.757	0.7
	180	3.228	3.205	0.7
* $\theta = 0$ corresponds to the back-scattered direction.				

NASTRAN structural model can be adapted for NASHUA acoustic analysis within a few hours.

One of the major benefits of having NASHUA linked with NASTRAN is the ability to integrate the acoustic analysis of a structure with other dynamic analyses. Thus the same finite element model can be used for modal analysis, frequency response analysis, linear shock analysis, and underwater acoustic

analysis. In addition, many of the pre- and postprocessors developed for use with NASTRAN become available for NASHUA as well.

The principal area in which NASHUA could be improved would be to remove the frequency limitation caused by the presence of the critical frequencies inherent in the Helmholtz integral equation formulation. With the limitation, cylindrical shells, for example, can be safely analyzed by NASHUA only for  $ka < 2.4$ , where  $a$  is the radius. Since for some problems, it would be of interest to treat higher frequencies, the limitation should be removed. A conversion to a different formulation (e.g., Burton and Miller [8] or Mathews [10]) is being considered.

#### REFERENCES

1. Everstine, G.C., "A Symmetric Potential Formulation for Fluid-Structure Interaction," J. Sound and Vibration, vol. 79, no. 1, pp. 157-160 (1981).
2. Everstine, G.C., "Structural-Acoustic Finite Element Analysis, with Application to Scattering," Proc. 6th Invitational Symposium on the Unification of Finite Elements, Finite Differences, and Calculus of Variations, ed. by H. Kardestuncer, Univ. of Connecticut, pp. 101-122 (1982).
3. Kalinowski, A.J., and C.W. Nebelung, "Media-Structure Interaction Method," The Shock and Vibration Bulletin, vol. 51, part 1, pp. 173-193 (1981).
4. Chen, L.H., and D.G. Schweikert, "Sound Radiation from an Arbitrary Body," J. Acoust. Soc. Amer., vol. 35, no. 10, pp. 1626-1632 (1963).
5. Schenck, H.A., "Improved Integral Formulation for Acoustic Radiation Problems," J. Acoust. Soc. Amer., vol. 44, no. 1, pp. 41-58 (1968).
6. Henderson, F.M., "A Structure-Fluid Interaction Capability for the NASA Structural Analysis (NASTRAN) Computer Program," Report 3962, David Taylor Naval Ship R&D Center, Bethesda, Maryland (1972).
7. Wilton, D.T., "Acoustic Radiation and Scattering From Elastic Structures," Int. J. Num. Meth. in Engrg., vol. 13, pp. 123-138 (1978).
8. Burton, A.J., and G.F. Miller, "The Application of Integral Equation Methods to the Numerical Solution of Some Exterior Boundary-Value Problems," Proc. Roy. Soc. Lond. A, vol. 323, pp. 201-210 (1971).
9. Baron, M.L., and J.M. McCormick, "Sound Radiation from Submerged Cylindrical Shells of Finite Length," ASME Trans. Ser. B, vol. 87, pp. 393-405 (1965).

10. Mathews, I.C., "A Symmetric Boundary Integral-Finite Element Approach for 3-D Fluid Structure Interaction," in Advances in Fluid-Structure Interaction - 1984, PVP-Vol. 78 and AMD-Vol. 64, ed. by G.C. Everstine and M.K. Au-Yang, American Society of Mechanical Engineers, New York, pp. 39-48 (1984).
11. Everstine, G.C., F.M. Henderson, E.A. Schroeder, and R.R. Lipman, "A General Low Frequency Acoustic Radiation Capability for NASTRAN," Fourteenth NASTRAN Users' Colloquium, NASA CP-2419, National Aeronautics and Space Administration, Washington, DC, pp. 293-310 (1986).
12. Lamb, H., Hydrodynamics, sixth edition, Dover Publications, New York (1945).
13. Lipman, R.R., "Computer Animation of Modal and Transient Vibrations," NASTRAN Users' Colloquium, National Aeronautics and Space Administration, Washington, DC (1987). (this volume)
14. Everstine, G.C., "A Portable Interactive Plotter for Digital X-Y Data," Report CMLD-86-45, David Taylor Naval Ship R&D Center, Bethesda, Maryland (1986).
15. Lipman, R.R., "Calculating Far-Field Radiated Sound Pressure Levels from NASTRAN Output," Fourteenth NASTRAN Users' Colloquium, NASA CP-2419, National Aeronautics and Space Administration, Washington, DC, pp. 282-292 (1986).
16. Junger, M.C., and D. Feit, Sound, Structures, and Their Interaction, second edition, The MIT Press, Cambridge, Massachusetts (1986).
17. Huang, H., and Y.F. Wang, "Asymptotic Fluid-Structure Interaction Theories for Acoustic Radiation Prediction," J. Acoust. Soc. Amer., vol. 77, no. 4, pp. 1389-1394 (1985).
18. Huang, H., "Helmholtz Integral Equations for Fluid-Structure Interaction," Advances in Fluid-Structure Interaction - 1984, AMD-Vol. 64, ed. by G.C. Everstine and M.K. Au-Yang, American Society of Mechanical Engineers, New York (1984).